

Definitions of entanglement entropy of spin systems in the valence-bond basis

Yu-Cheng Lin¹ and Anders W. Sandvik²

¹*Graduate Institute of Applied Physics, National Chengchi University, Taipei, Taiwan*

²*Department of Physics, Boston University, 590 Commonwealth Avenue, Boston, Massachusetts 02215, USA*

(Dated: July 30, 2018)

The valence-bond structure of spin-1/2 Heisenberg antiferromagnets is closely related to quantum entanglement. We investigate measures of entanglement entropy based on transition graphs, which characterize state overlaps in the overcomplete valence-bond basis. The transition graphs can be generated using projector Monte Carlo simulations of ground states of specific hamiltonians or using importance-sampling of valence-bond configurations of amplitude-product states. We consider definitions of entanglement entropy based on the bonds or loops shared by two subsystems (bipartite entanglement). Results for the bond-based definition agrees with a previously studied definition using valence-bond wave functions (instead of the transition graphs, which involve two states). For the one dimensional Heisenberg chain, with uniform or random coupling constants, the prefactor of the logarithmic divergence with the size of the smaller subsystem agrees with exact results. For the ground state of the two-dimensional Heisenberg model (and also Néel-ordered amplitude-product states), there is a similar multiplicative violation of the area law. In contrast, the loop-based entropy obeys the area law in two dimensions, while still violating it in one dimension—both behaviors in accord with expectations for proper measures of entanglement entropy.

PACS numbers: 75.10.Jm, 02.70.Ss, 75.40.Mg, 03.65.Ud

I. INTRODUCTION

The concept of quantum mechanical entanglement is of broad interest in physics. One widely used quantitative measure of entanglement is the von Neumann entanglement entropy S_{vN} . Partitioning a many-body system in a pure quantum state into two contiguous subsystems, S_{vN} is defined as the von Neumann entropy of the reduced density matrix of either one of the two subsystems. The insight that S_{vN} typically scales proportionally to the boundary area (the area law¹) was first developed in the context of black holes.² The area law has now become a key benchmark for characterizing states of interest in quantum information theory^{3,4} and condensed matter physics.^{5,6} An important application of this concept is to construct computationally tractable variational ansätze for ground states based on the area law.^{7,8}

While S_{vN} is a clear and well established measure of entanglement, it is difficult to compute for strongly-correlated quantum systems in dimensions higher than one, where exact diagonalization and density matrix renormalization group approaches become inefficient.^{9,10} Alternative definitions of entanglement entropy (or, more precisely, alternative measures of entanglement) are therefore also actively investigated. The Rényi entropies S_n ($n = 1, 2, \dots$) are often used,¹¹ and have the appealing property that $S_1 = S_{\text{vN}}$. Recently it was realized¹² that S_2 (and in principle also S_n for $n > 2$) can be computed for quantum spin systems using projector quantum Monte Carlo (QMC) simulations in the valence bond (VB) basis.¹³ Previously, a measure S_{VB} of entanglement entropy explicitly making use of the VB basis was also introduced^{14,15} within the context of this QMC method. Generalizing an exact result for a single VB state¹⁶ to a superposition, S_{VB} is given by the average number

of VBs connecting two subsystems. While defined explicitly using the VB basis, this quantity also can be evaluated using the density matrix renormalization group (DMRG) method¹⁷ and is, therefore, not completely tied to the VB basis. Its asymptotic behavior has also been found exactly using analytical methods for the Heisenberg chain.¹⁸

In this paper, we formulate a different measure S_{VB}^2 of entanglement entropy for quantum spin systems in terms of the transition graphs characterizing overlaps of VB basis states. The transition graphs are generated in projector Monte Carlo simulations of the ground state of a hamiltonian,^{13,19} or in Monte Carlo sampling of bond configurations of variational states such as the amplitude product states.^{19,20} Like the previous definition of VB entanglement entropy, which we henceforth call S_{VB}^1 , the transition-graph definition S_{VB}^2 involves VBs shared by two subsystems, but the weighting is different because the bond configurations in the projected bra and ket states are sampled using their individual wave functions and overlap (which depends on the number of loops in the transition graph). We show that S_{VB}^2 scales with the subsystem size in accord with an exact result¹⁸ for the previous definition S_{VB}^1 in the one dimensional (1D) Heisenberg chain. The corrections to this form are much smaller than in the previous definition, however. Thus, the different weighting procedure appears to reduce the subleading size corrections.

Both S_{VB}^1 and S_{VB}^2 violate the area law in the case of the Néel-ordered ground state of the two-dimensional (2D) Heisenberg model. We here argue that this is because definitions based on single VBs typically will overestimate the entanglement, due to the over-completeness of the VB basis. To remedy this, we propose an alternative measure S_{loop} of entanglement entropy based on

the loops of the transition graphs, i.e., S_{loop} is the average number of transition-graph loops shared by the two subsystems. Loops correspond to maximally entangled groups of spins, and the number of loops shared by the subsystems is therefore an appropriate measure of entanglement. We show that S_{loop} of the 2D Heisenberg model (and also in a generic variational amplitude-product state with Néel order) obeys the area law and has an additive logarithmic correction, in contrast to the multiplicative logarithmic corrections affecting the bond-based definitions. Thus, it appears that the loop entropy scales in the same way as the Rényi entropy (as observed in Ref. 12) and the standard von Neumann entanglement entropy (where one would expect such scaling) and, thus, may be a convenient (more easily computable) stand-in for these definitions.

The outline of the rest of the paper is as follows. In Sec. II we summarize the properties of the VB basis needed for our definitions and calculations, and also briefly review amplitude-product states,²⁰ the VB projector QMC method,^{13,19} and the loop-gas picture^{21,22} of VB states. The VB and loop entropy definitions are discussed and tested in Secs. III and IV. We conclude in Sec. V with a summary and discussion.

II. VALENCE-BOND BASIS AND METHODS

We will consider the spin-1/2 Heisenberg hamiltonian, written in the form

$$H = - \sum_{\langle i,j \rangle} J_{ij} S_{ij}, \quad (J_{ij} > 0), \quad (1)$$

where $\langle i,j \rangle$ denotes nearest-neighbor spins on a lattice with periodic boundaries and S_{ij} is a singlet projector,

$$S_{ij} = 1/4 - \mathbf{S}_i \cdot \mathbf{S}_j, \quad (2)$$

and $J_{ij} > 0$ are antiferromagnetic coupling constants. We will study 1D chains with uniform and random couplings, as well as uniform 2D square lattices.

Here, in Sec. II A, we discuss the VB basis in which we carry out all calculations. In Sec. II B we discuss variational VB amplitude-product states, which give some important insights into various types of ground states and their entanglement properties. The projector QMC calculations that we use for unbiased calculations are briefly reviewed in Sec. II C. The loop-gas picture of VB states was first introduced by Sutherland.^{21,22} In Sec. II D we discuss it in a somewhat broader sense, which we will rely on for the definition of loop entropy in Sec. IV.

A. The valence-bond basis

The ground state of H on a bipartite lattice with an even number N of spins is a total-spin singlet and can be expanded in bipartite VB states (i.e., each bond

connects sites on the two sublattices) with all positive coefficients;²⁰

$$|\psi_0\rangle = \sum_v \lambda_v |v\rangle, \quad (\lambda_v \geq 0 \forall v). \quad (3)$$

With the singlet state of two spins i, j denoted by (i, j) , a bipartite VB basis state is defined as

$$|v\rangle := \bigotimes_{ij} (i, j), \quad (i, j) := \frac{1}{\sqrt{2}} (|\uparrow_i \downarrow_j\rangle - |\downarrow_i \uparrow_j\rangle), \quad (4)$$

where sites i and j are on different sublattices and each site appears exactly once in the product. Thus, there are $(N/2)!$ different basis states $|v\rangle$ which form an over-complete basis in the singlet subspace.

The overlap $\langle v'|v\rangle$ between two VB basis states can be expressed in terms of transition-graph loops, as illustrated in Fig. 1. Each lattice site is connected to one bond from $|v\rangle$ and one from $\langle v'|$, and all the bonds therefore form closed loops. The matrix element $\langle v'|v\rangle$ is a product of factors arising from these loops. To evaluate $\langle v'|v\rangle$ it is more convenient to work in the standard spin- z basis and rewrite a VB state $|v\rangle$ as

$$|v\rangle = \frac{1}{2^{N/4}} \sum_{\alpha=1}^{2^{N/2}} (-1)^{n_{\mathcal{B}\uparrow}} |S_1^z, S_2^z, \dots, S_N^z\rangle_{\alpha}, \quad (5)$$

where α labels the spin states that are compatible with the valence bonds in $|v\rangle$ (i.e., $\uparrow\downarrow$ or $\downarrow\uparrow$ spin configurations on each bond) and $n_{\mathcal{B}\uparrow}$ is the number of \uparrow spins on sublattice \mathcal{B} , the sign following if the singlet (4) is defined such that i and j are on sublattices \mathcal{A} and \mathcal{B} , respectively (which corresponds to Marshall's sign rule²³ for a bipartite system). From the orthonormality of the ordinary basis of states $\{|S_1^z, S_2^z, \dots, S_N^z\rangle\}$, the only nonzero terms in $\langle v'|v\rangle$ expressed using (5) are those with spin configurations common to both the VB states $|v\rangle$ and $\langle v'|$. This corresponds to spins forming staggered patterns, $\uparrow\downarrow\uparrow \dots \downarrow$ or $\downarrow\uparrow\downarrow \dots \uparrow$, around each loop. There are two such staggered configurations of each loop and the signs in (5) cancel in the overlap, which, thus, is given by²¹

$$\langle v'|v\rangle = 2^{N_o - N/2}, \quad (6)$$

where N_o is the number of loops in the transition graph. This is illustrated in Fig. 1.

In the VB description many physically quantities are determined by the statistical properties of the transition-graph loops. For instance, the normalized matrix element needed for computing the spin-spin correlation function is given by

$$\frac{\langle v' | \mathbf{S}_i \cdot \mathbf{S}_j | v \rangle}{\langle v' | v \rangle} = \begin{cases} \pm 3/4, & [i, j], \\ 0, & [i][j], \end{cases} \quad (7)$$

where $[i, j]$ and $[i][j]$ denote sites i and j belonging to the same loop and different loops, respectively, and the sign

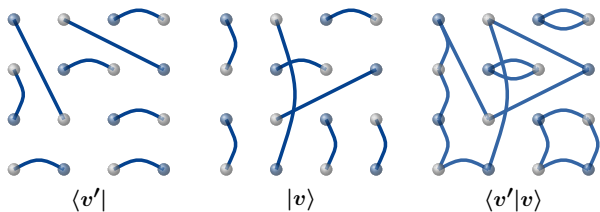


FIG. 1: (Color online) Transition graph (right) determining the overlap of two VB states $|v\rangle$ and $|v'\rangle$. Note that in the restricted VB basis considered here, all bonds connect sites on different sublattices (with sites on sublattices \mathcal{A} and \mathcal{B} here indicated by darker and lighter circles). The cluster of spins defined by a loop can be in two states, with all spins \uparrow on sublattice \mathcal{A} and \downarrow on \mathcal{B} , or vice versa.

in the case $[i, j]$ is $+$ and $-$ for spins on the same and different sublattices, respectively.

Note that the transition graph loops define clusters of spins that do not necessarily resemble geometric loops on the lattice, because the VBs can be of any length and the bonds forming a loops can cross each other (as seen in Fig. 1). Note also that the staggered spin configuration along a loop also corresponds to staggering of all spins in the loop in the sense of the two sublattices, i.e., all spins on sublattice \mathcal{A} are parallel and opposite to those on \mathcal{B} . This is the origin of the signs in (7).

B. Amplitude-product states

In an amplitude-product state,²⁰ the expansion coefficients in (3) are products of amplitudes $h(\mathbf{r}_{ij}) > 0$ (to maintain Marshall’s sign rule for the ground state of a bipartite model),

$$\lambda_v = \prod_{(i,j)} h(\mathbf{r}_{ij}), \quad (8)$$

with the vector \mathbf{r}_{ij} denoting the “shape” (the lengths in all lattice dimensions) of bond (i, j) in $|v\rangle$. This form applies to a translationally invariant system, while in a non-uniform system one should use $h(\mathbf{r}_i, \mathbf{r}_j)$ depending on both end-points of the bonds.

For a given set of amplitudes, the expectation value of some operator O can be written as

$$\langle O \rangle = \frac{\langle \psi_0 | O | \psi_0 \rangle}{\langle \psi_0 | \psi_0 \rangle} = \frac{\sum_{vv'} W_{vv'} \frac{\langle v' | O | v \rangle}{\langle v' | v \rangle}}{\sum_{vv'} W_{vv'}}, \quad (9)$$

where the configuration weight is given by

$$W_{vv'} = \lambda_v \lambda_{v'} \langle v' | v \rangle = \lambda_v \lambda_{v'} 2^{N_0 - N/2}. \quad (10)$$

The ratio $\langle v' | O | v \rangle / \langle v' | v \rangle$ can normally be related to the loop structure of the transition graph,^{20,24} e.g., Eq. (7) in the case of a spin correlation function.

The expectation value (9) is ideally suited for evaluation using Monte Carlo sampling methods,^{19,20} and all

the amplitudes can be variationally optimized.^{19,25} Calculations for the Néel-ordered ground state of the 2D Heisenberg model suggest that the fully optimized amplitudes decay as a power-law, $h(|\mathbf{r}_{ij}|) = 1/|\mathbf{r}_{ij}|^p$, with $p \approx 3$.^{19,25} There is reason to believe that the decay exponent in fact is exactly $p = 3$, as this is the exponent obtained in an analytical mean-field-like treatment.²⁶ Some aspects of the critical 1D chain can also be captured with amplitude-product states.²⁷

The properties of quantum systems are often modified dramatically by introducing quenched (static) randomness: e.g., quantum phase transitions with disorder can lead to new universality classes. For the Heisenberg chain, it is known that any amount of quenched randomness will drive the system into a state well approximated by a random singlet state—a single VB basis state (which is of the “nested” type, with no crossing VBs) with arbitrary VB lengths obtained according to a strong-disorder renormalization-group (SDRG) scheme.^{28–30} In this case, the transition-graph loops coincide exactly with the VBs, i.e., $N_0 = N/2$ in (6), and many asymptotic properties follow directly from the length distribution of the VBs.

Amplitude-product states (as well as the special case of the SDRG random singlet states) are useful variational states and we will consider some aspects of their entanglement properties. In many cases completely unbiased results are needed, however. One way to achieve this is with projector QMC simulations in the VB basis, which we briefly discuss next.

C. Projector QMC method

In the VB QMC method^{13,31} the ground state of the hamiltonian (1) is projected out stochastically, by applying a high power of H to some trial singlet state $|\psi_t\rangle$ in the VB basis; $(-H)^m |\psi_t\rangle \rightarrow |\psi_0\rangle$ for a large m (up to an irrelevant normalization). A good trial state, such as an optimized amplitude-product state for a uniform system or a single VB state obtained with the SDRG procedure for a 1D random chain, can be used to optimize the convergence properties of such a scheme, but the final result is not sensitive to $|\psi_t\rangle$ as long as m is sufficiently large (i.e., the method is unbiased).

There are two formulations of the VB QMC method,¹³ generating either the ground state wave function or the ket and bra versions of the ground state needed to evaluate expectation values. In the former case, stochastic application of the projector H^m (for sufficiently large m) on the trial state produces VB basis states distributed proportionally to the expansion coefficients λ_v in (3), i.e., these coefficients are not known (and would be much more complicated than the simple amplitude products) but importance-sampling of the contributions to $H^m |\psi_t\rangle$, which resemble terms in a path integral, generate them probabilistically (with many paths contributing to a single coefficient λ_v).

In the “double projection” method, an expectation

value is formally given by Eq. (9), but the expansion coefficients λ_v are again not known. The sampling of paths obtained from the combined ket $H^m |\psi_t\rangle$ and bra $\langle\psi_t| H^m$ states, i.e., $\langle\psi_t| H^{2m} |\psi_t\rangle$, leads to a series of VB-pair configurations distributed according to the weights $W_{vv'}$ in (10).

In both the wave-function and expectation-value projection schemes, one can employ efficient loop updates for generating the states and transition graphs, as discussed in detail in Ref. 19. In the sampling procedures of such algorithms, one uses the combined spin-bond basis and applies a high power H^m or H^{2m} in a way similar to the "operator-loop" update in the finite temperature stochastic series expansion QMC method.³² The computational effort scales as $\mathcal{O}(m)$, and to converge calculated quantities to the ground state m has to be scaled as $\propto N^a$, with a typically in the range $1 - 2$ (depending on the model's low-energy energy spectrum and the quality of the trial state $|\psi_t\rangle$).¹⁹

D. Loop-gas description

The loop-gas view of VB sampling was suggested by Sutherland some time ago.^{21,22} Consider the two VB configurations in a transition graph $\langle v'|v\rangle$ with the associated weight (10) for an amplitude-product state. In that case, the factor $\lambda_v \lambda_{v'}$ does not depend on details of the bond arrangements, only on the total number $N_b(\mathbf{r})$ of bonds of all shapes \mathbf{r} in the two states $|v\rangle$ and $|v'\rangle$ (i.e., no bond correlations are included). In addition to the factor 2 in the overlap (6) for each loop in the transition graph, for each loop containing more than two bonds we can consider swapping all bonds belonging to a given loop between $|v\rangle$ and $|v'\rangle$, as illustrated in Fig. 2. This swapping does not affect the weight (10) of the joint configuration of the two states (although the weights λ_v and $\lambda_{v'}$ of the individual states are affected). The two bond configurations and two staggered spin patterns for each loop corresponds to a loop fugacity 4 for all loops of length 4 or larger. The shortest, length-2, loops have fugacity 2, as the bond swapping in this case does not affect the bond configurations.

Instead of sampling bonds weighted according to (10), one can think of sampling loops with the weight

$$W = 2^{N_o(2)} 4^{N_o(>2)} \prod_{\mathbf{r}} h(\mathbf{r})^{N_b(\mathbf{r})}, \quad (11)$$

where $N_o(2)$ and $N_o(>2)$ denote the number of loops of length 2 and larger than 2, respectively, and the unimportant factor $2^{-N/2}$ in (6) has been omitted. The product of amplitudes can here be thought of as originating from the shapes of the loops. In special cases, such as Anderson's resonating valence-bond (RVB) state including only the shortest bonds (of length $r = 1$),³³⁻³⁵ the weight only depends on the number of loops. This was the case considered by Sutherland,²² who also studied generalizations of the loop gas in which the loop fugacities, $Z_2 = 2$

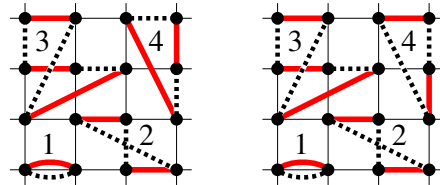


FIG. 2: (Color online) Two transition graphs $\langle v'|v\rangle$ with the same loops structure (with four loops, labeled 1,2,3,4). The two cases shown here illustrate how bonds within a loop (here loop 4) can be swapped between $|v\rangle$ and $\langle v'|$ (represented by solid and dashed bonds, respectively). This kind of bond reconfiguration leaves the weight unchanged in the case of an amplitude-product state, but not in a more general state in which there are correlations between the bonds.

and $Z_{>2} = 4$ in (11), can take arbitrary values and, thus, phase transitions can be studied as a function of these fugacities.

The loop-gas weight function (11) does not apply to states beyond the amplitude-product description. In the exact ground state of a given hamiltonian, one would in general expect bond correlations. The product of two VB expansion coefficients in (10) then changes when an intra-loop bond swap of the type illustrated in Fig. 2 is carried out, thus invalidating the form (11). One can still, however, sum up the weights obtained as a result of all such bond swaps which leave the loop structure intact, and this way, in principle (but hardly in practice), write down a weight for a loop configurations which is more complicated than (11). The loop configurations generated in the QMC projector method represent a stochastic implementation of this more general loop-gas picture. Note that even in this generalization, each loop is associated with a factor of two arising from the two allowed staggered spin configurations of the cluster of sites defined by the loop.

III. VALENCE-BOND ENTANGLEMENT ENTROPY

A singlet state formed by two $S = 1/2$ spins is maximally entangled and has the maximum value of the von Neumann bipartite entanglement entropy; $S_{\text{VN}} = 1$ (measured in bits). The simplest case for computing S_{VN} of a many-body system is a single VB basis state $|v\rangle$. For a given bipartition, its entanglement entropy is just the number of singlets n_{AB} connecting subsystems \mathcal{A} and \mathcal{B} .¹⁶ It is not easy to compute S_{VN} for a superposition of VB states, however. In Refs. 14 and 15 a straightforward generalization of the result for a single VB state was proposed as an alternative definition of entanglement entropy for an arbitrary superposition of VB states, using the average number of bonds connecting the two subsystems. With the VB projector method for the wave

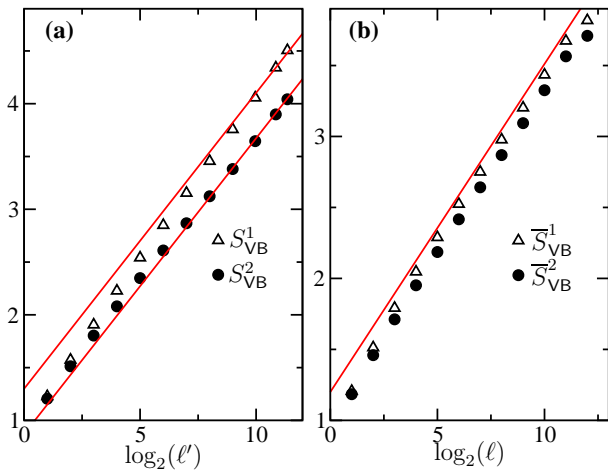


FIG. 3: (Color online) (a) VB entropies for subsystems of size ℓ in a Heisenberg chain of length $L = 2^{13}$ as a function of the logarithm of the conformal distance; $\log_2(\ell') = \log_2[(L/\pi) \sin(\pi\ell/L)]$. The lines have slope $\gamma = 4 \ln(2)/\pi^2$, as in the exact asymptotic form.¹⁸ (b) Disorder-averaged VB entropies for the 1D random chain, as a function of $\log_2(\ell)$. The line has slope $\gamma = \ln(2)/3$.

function, one stochastically evaluates

$$S_{\text{VB}}^1 = \frac{\sum_v \lambda_v n_{AB}}{\sum_v \lambda_v}. \quad (12)$$

Here we investigate a different definition, using the expectation value

$$S_{\text{VB}}^2 = \langle n_{AB} \rangle, \quad (13)$$

evaluated using Eq. (9) with $O = n_{AB}$. Here it should be noted that we define n_{AB} as just counting of the bonds crossing the two subsystems, and that this counting can be performed in the transition graph of $\langle v'|v \rangle$ either in $|v\rangle$ or $\langle v'|$. For a given configuration these numbers are different (i.e., the operator is not hermitian), but the averages are the same. In Sec. V we will address further potential problems in interpreting $\langle n_{AB} \rangle$ as a standard quantum mechanical expectation value. For now, we consider this quantity as an interesting aspect of the transition graphs, the statistical properties of which are uniquely determined for a given hamiltonian with short-range interactions (as we will further argue in Sec. V).

For a single VB state $S_{\text{VB}}^2 = S_{\text{VB}}^1$, but in a superposition these quantities are different, because of the over-completeness and associated different weighting of the VB configurations. We next present projector QMC results for both S_{VB}^1 and S_{VB}^2 in 1D and 2D Heisenberg systems and discuss their scaling as a function of the size of the smaller subsystem of the bipartition.

A. Homogeneous chain

We consider first the standard Heisenberg chain with uniform interactions. For a large segment of size ℓ , em-

bedded in a chain of length L , the von Neumann entanglement entropy has the asymptotic behavior $S_{\text{vN}}(\ell) = (c/3) \log_2(\ell') + s_0$, where $\ell' = (L/\pi) \sin(\pi\ell/L)$ is the conformal length, $c = 1$ is the central charge, and s_0 is a non-universal constant.³⁶ The VB entropy S_{VB}^1 is known to diverge in the same way, but with a different factor, $\gamma = 4 \ln(2)/\pi^2 \approx 0.281$.¹⁸ Previous calculations are consistent with $\gamma < 1/3$ for large chains,¹⁰ but, as can be seen in Fig. 3(a) for a chain of 2^{13} spins, there are still large non-asymptotic corrections which make it difficult to verify the factor precisely.¹⁷ On the other hand, our results for S_{VB}^2 are completely consistent with the known γ over a large range of subsystems. This may appear surprising, because the exact calculation is based on the wave-function definition S_{VB}^1 ,¹⁸ not the expectation value S_{VB}^2 . It is plausible, however, that S_{VB}^1 and S_{VB}^2 scale asymptotically with the same γ (with different additive constants), but that S_{VB}^2 is less affected by subleading scaling corrections.

B. Disordered chain

Now we turn to the disordered chain, with random couplings generated from the uniform distribution in the interval $(0, 1]$. The ground state of this system is known to be well approximated by a random singlet, where all spins form a single non-crossing VB state with arbitrary bipartite bond lengths.²⁹ Using an SDRG analysis, Refael and Moore¹⁶ showed that the disorder average of the von Neumann entanglement entropy \bar{S}_{vN} in such a state scales logarithmically with a universal coefficient $\gamma = \ln(2)/3$. This result should hold also for the VB entanglement entropy of the Heisenberg chain when $L \rightarrow \infty$, although the ground state is not exactly a single VB basis state—there are fluctuations around the dominant SDRG configuration.³⁷ Our results for both S_{VB}^1 and S_{VB}^2 , shown in Fig. 3(b), are consistent with $\gamma = \ln(2)/3$ (considering some remaining finite-size effects for the largest subsystems).

C. Two-dimensional system

We next consider the 2D Heisenberg model, which we have studied on $L \times L$ lattices with L up to 256. Fig. 4 shows results for $S_{\text{VB}}^2(\ell)$ of square subsystems of linear size ℓ . The data converge very rapidly with L for $\ell \leq L/4$. There is clearly a multiplicative logarithmic correction to the area law, $S_{\text{VB}}^2(\ell)/\ell \propto \log_2(\ell)$, as found previously for S_{VB}^1 in Refs. 10,14. Both VB entropy definitions, thus, violate the area law in this case. The von Neumann entropy, on the other hand, should obey the area law, $S_{\text{vN}}(\ell) \propto \ell$, although, because of difficulties in calculating this quantity in an unbiased way, it has not been possible to confirm it unambiguously.¹⁰ The recent calculation of the Rényi entropy S_2 is, however, in agreement with the area law.¹²

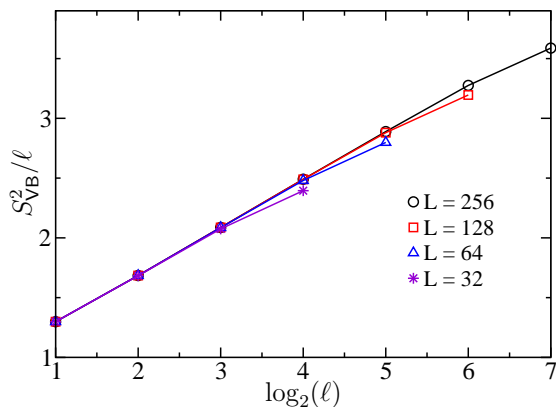


FIG. 4: (Color online) The VB entropy S_{VB}^2 divided by the linear dimension ℓ of a square sub-block in 2D $L \times L$ lattices with $L = 32 - 256$.

We conclude that S_{VB}^2 has an advantage over S_{VB}^1 , in the sense that its logarithmic prefactor in 1D converges faster to the result of the exact calculation in Ref. 18 (although we do not know whether the faster convergence is generic). Neither of these definitions serves well as a proxy for the von Neumann entanglement entropy S_{vN} , however, because the area law is violated in 2D by a multiplicative logarithmic correction. Only additive corrections to the area law are expected.^{38,39}

IV. LOOP ENTANGLEMENT ENTROPY

The loop-gas picture discussed in Sec. IID suggests a potential reason why the VB entanglement entropies (12) and (13) violate the area law in 2D systems: The VB basis consists of singlet pairs, but when considering an expectation value, constraints related to the overcompleteness are imposed on the spin states beyond the singlet pairing. These constraints are similar to multi-spin entanglement, as there are two spin states for each loop (the two staggered spin configurations on the loops) and these loops are, thus, analogous to maximally entangled sets of spins (albeit in an overlap matrix element, not a wave function). All bonds therefore do not carry a full unit of entanglement entropy (because they are entangled with other bonds in the same loop), and the VB entropy S_{VB}^2 may therefore overestimate the actual entanglement entropy. This could also be the case with S_{VB}^1 , because it, too, is based on a superposition of states with only pair-wise entanglement (and, as we showed in Sec. III, S_{VB}^1 and S_{VB}^2 have the same scaling properties). On the other hand, in 1D S_{VB}^1 and S_{VB}^2 actually underestimate the entanglement entropy (in relation to the von Neumann entanglement entropy, which is slightly larger than the bond entropies in this case). The intuitive picture of entanglement entropy in terms of bonds is therefore, as a consequence of the overcompleteness, not always quantitatively correct.

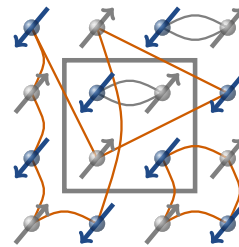


FIG. 5: (Color online) The loop entropy S_{loop} of a subsystem (gray square) is defined as the average number of loops in the transition graph shared by the subsystem and the rest of the system. In this example two loops are shared.

We will here consider a measure of entanglement entropy S_{loop} in terms of shared loops in the transition graph, as illustrated in Fig. 5. Since the number of shared loops must be smaller or equal to the number of shared bonds, we have $S_{\text{loop}} \leq S_{\text{VB}}^2$, and it is therefore clear that S_{loop} cannot be a better approximation to S_{vN} than S_{VB}^2 in the case of the 1D Heisenberg chain. We will be mainly interested in S_{loop} of the 2D system, but will also investigate it in 1D.

Before discussing the actual definition of S_{loop} further, let us consider for a moment the wave function. Instead of a bond-singlet pairing of the spins, one might regard a state as a superposition of products of loop-cluster states,

$$|\Psi\rangle = \sum_{\alpha} \bigotimes_{i=1}^{N_{\alpha}} |\psi(i)\rangle_{\alpha}, \quad (14)$$

where N_{α} is the number of loops in component α and an individual cluster state of n spins is of the form

$$|\psi(i)\rangle_{\alpha} = \frac{1}{\sqrt{2}} \left(|\uparrow_1 \downarrow_2 \cdots \downarrow_n\rangle_{\alpha} - |\downarrow_1 \uparrow_2 \cdots \uparrow_n\rangle_{\alpha} \right). \quad (15)$$

This is a maximally entangled state of two staggered spin configurations along the loop of n spins (or, equivalently, all even numbered spins are on sublattice \mathcal{A} and all odd ones on \mathcal{B} , or vice versa). With such a loop-cluster wave function, it is natural to regard a loop shared by two subsystems in a bipartition as carrying one unit of entanglement entropy. Thus, we define the *loop entanglement entropy* as

$$S_{\text{loop}} = \langle \Lambda_{AB} \rangle, \quad (16)$$

where Λ_{AB} counts the number of loops shared by subsystems A and B (i.e., loops passing through both the subsystems) in a given bipartition.

The loop-cluster view of entanglement entropy is realized in SDRG calculations for the random transverse-field Ising model,⁴⁰ where the clusters have parallel spins and the ground state is given by a single product of such cluster states. The generalization to a superposition of cluster products has the same motivation as the generalization of the entanglement entropy of the single VB state

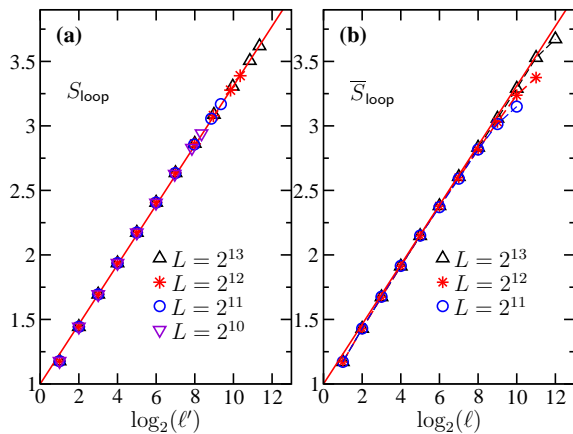


FIG. 6: (Color online) Loop entropy of Heisenberg chains with (a) uniform and (b) random couplings (versus the logarithms of the conformal and linear subsystem sizes, respectively). Both lines have slope $\gamma = \ln(2)/3$.

appearing in the SDRG scheme for the random Heisenberg chain¹⁶ to a superposition.^{14,15} In general, it is not known, however, how to write the wave function of a Heisenberg system as a superposition of cluster states (and clearly there is no unique way of doing so, as such a basis is massively overcomplete). As we have seen, such loop-cluster superpositions do appear in the loop-gas picture, and it is then natural to define S_{loop} as above using the transition graph loops, as illustrated in Fig. 5. We will explore this measure of entanglement here.

One may again question whether an expectation value such as $\langle \Lambda_{AB} \rangle$ is a *bona fide* quantum mechanical expectation value. We will discuss this further in Sec. V and here only consider it, like S_{VB}^2 , as a statistical property of the transposition graphs generated in the projector QMC scheme (or in sampling of an amplitude-product state, which we will also investigate).

Clearly, the loop entropy is a boundary property, and we can write either $S_{\text{loop}}(A)$ or $S_{\text{loop}}(B)$ for a bipartition (A, B) . It is easy to demonstrate the sub-additive property $S_{\text{loop}}(A_1 \cup A_2) \leq S_{\text{loop}}(A_1) + S_{\text{loop}}(A_2)$ for two different bipartitions, (A_1, B_1) and (A_2, B_2) . The essential properties of an entropy are thus satisfied. For a single VB configuration, loops and bonds coincide and, thus, $S_{\text{loop}} = S_{\text{VB}}^1 = S_{\text{VB}}^2 = S_{\text{vN}}$ in this case.

A. 1D and 2D Heisenberg models

We first consider the loop entropy for ground states of Heisenberg models obtained by the projector QMC method. Figs. 6 and 7 show results for 1D and 2D systems, respectively. Interestingly, in 1D, the behavior is consistent with a logarithmic divergence with a prefactor $\gamma = \ln(2)/3 \approx 0.231$ (to within a statistical error of about 1%) for both the uniform and random chains (with uniformly distributed couplings between 0 and 1), i.e., the

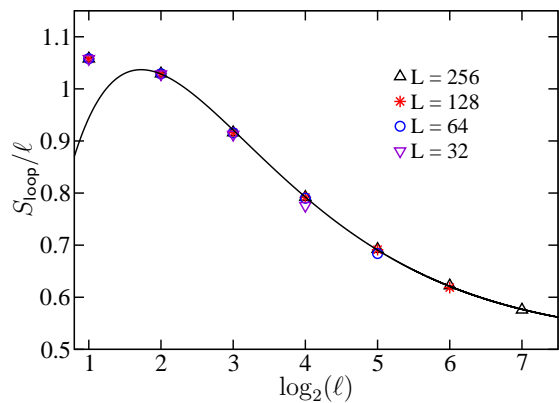


FIG. 7: (Color online) The loop entropy divided by the linear dimension ℓ of a square sub-block in several $L \times L$ lattices. The curve shows a fit of the $L = 256$ data ($\ell \geq 2^2$) to the form $S_{\text{loop}} = \mu\ell + a \log_2(\ell) + s_0$, with $\mu \approx 0.51$, $a \approx 1.12$, and $s_0 \approx -0.34$. The quality of this fit is statistically sound, with $\chi^2/\text{dof} < 1$ when $\ell \geq 8$ data are included. The error bars are much smaller than the symbols, of the order 10^{-4} for S_{loop}/ℓ .

same as the bond-based entropy for the random chain (Fig. 3). The result is expected for the random chain, because the asymptotic SDRG state of such a system is a single VB state, in which $S_{\text{loop}} = S_{\text{VB}}^1 = S_{\text{loop}}^2$ (and this is the exact result), but it is curious that the same value obtains for the uniform chain as well. This may also be taken as a flaw of the loop-based entropy (if one wants a quantity mimicking the von Neumann entropy as closely as possible), because it is further from S_{vN} ($\gamma = 1/3$) than the bond-based estimates ($\gamma = 4 \ln(2)/\pi^2 \approx 0.281$). Nevertheless, it is encouraging that the logarithmic divergence is still captured.

In the 2D system, S_{loop}/ℓ converges to a finite value with increasing ℓ and L . Note the rapid convergence as a function of the full system size in Fig. 7. For the largest system ($L = 256$) the results are described very well by an area law with an additive logarithmic correction; $S_{\text{loop}} = \mu\ell + a \log_2(\ell) + s_0$. The area law prefactor $\mu \approx 0.51$ is, intriguingly, in good agreement with S_{vN}/ℓ obtained by Kallin *et al.*¹⁰ for wide ladder systems [accounting for the $\ln(2)$ included there in the definition of S_{vN}]. In this case the loop entropy is, thus, a better stand-in for S_{vN} (which is expected to obey the area law) than the bond-based quantities.

Note that the presence of long-range Néel order in 2D implies the existence of system-spanning loops in the transition graph.¹⁹ This explains why S_{loop} is much smaller than S_{VB}^2 in Fig. 5 (i.e., because of the large average loop size, the number of loops in the transition graph is much smaller than the number of bonds).

B. Néel-ordered 2D amplitude-product state

We also investigate the scaling behavior of the loop entropy for a 2D amplitude product state, (4) with the ex-

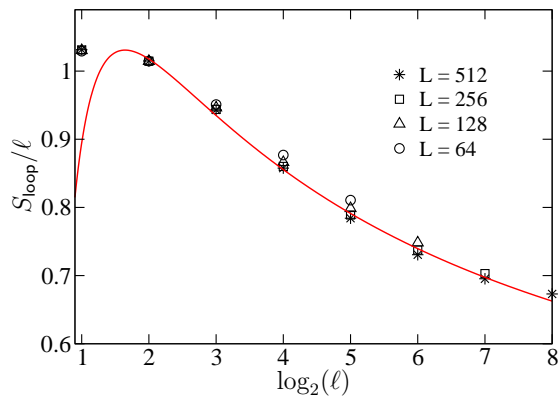


FIG. 8: (Color online). Loop entropy of the amplitude-product state with amplitudes decaying with the bond length r as $h(r) = 1/r^3$, which is the asymptotic form in the optimal amplitude product state for the 2D Heisenberg model.²⁵ The entropy divided by the system length saturates for large systems, indicating applicability of the area law (with an additive logarithmic correction described by the same form as in Fig. 7; a fit is indicated by the solid curve).

pansion coefficients given by (8) with $h(r) = 1/r^3$. This corresponds to the asymptotic form of the optimal variational amplitudes for the 2D Heisenberg model suggested by previous calculations.^{19,25} We here do not use fully optimized amplitudes (which show deviations from the $1/r^3$ for short bonds), because our aim is to investigate a generic Néel-ordered state, to compare with the results of the specific case of the ground state if the 2D Heisenberg model in Fig. 7.

The sublattice magnetization in the amplitude-product state with $h(r) = 1/r^3$ for all r is $m_s \approx 0.27$ (extracted from the system size dependence of $\langle m_s^2 \rangle$ for systems of size L up to 256), somewhat below the known value $m_s \approx 0.307$ for the Heisenberg model. The results in Fig. 8 show a behavior very similar to the Heisenberg ground state result in Fig. 7, with a correction to the area law which can be described as an additive logarithm. Because of the lower value of the sublattice magnetization, the average loop size is smaller, and, thus, the number of loops in the system (including those shared by the two subsystems) is larger, leading to higher overall value of S_{loop} than in Fig. 5.

V. SUMMARY AND DISCUSSION

Using the transition graphs characterizing state overlaps in the valence bond basis of $S = 1/2$ spins, we have explored two measures of bipartite entanglement entropy, S_{VB}^2 and S_{loop} . The former extends the definition S_{VB}^1 of valence-bond entropy (Refs. 14,15) based on shared valance bonds in the wave function to the transition graph, while the latter is based on shared loops (motivated by the loop-gas picture^{21,22} of spin systems). Using an efficient loop algorithm,¹⁹ we were able to ob-

tain unbiased QMC results for these quantities in large systems; 2^{13} and 2^{16} spins in 1D and 2D, respectively.

In the Heisenberg chain, S_{VB}^2 exhibits a logarithmic divergence, with a prefactor which agrees well with the exact value¹⁸ $\gamma = 4 \ln(2)/\pi^2$ already for small subsystems. In contrast, observing this scaling with the wavefunction definition S_{VB}^1 ^{10,14} requires very large systems, due to significant subleading corrections.¹⁷

For the Néel state of the 2D Heisenberg model, both VB entropies violate the area law, exhibiting multiplicative logarithmic corrections.¹⁴ We have argued that single-bond definitions typically overestimate the amount of entanglement, because of the over-completeness of the VB basis. The loop definition S_{loop} exhibits only an additive size correction to the area law in 2D, in agreement with general expectations for standard definitions.^{12,38,39}

Important relationships have been established in recent years between the subleading behavior of the entanglement entropy, topological order, and quantum-criticality. For instance, the subleading term in a 2D gapped system is a constant determined by the quantum dimension of the excitations of the topological phase.^{3,5} For critical systems in the universality class of $z = 2$ conformal quantum-critical points, there is a universal additive logarithmic subleading term, which depends only on the shape of the subsystem partition and the central charge.⁶ An additive correction to the area law in the 2D Néel state was also found for the Rényi entropy S_2 , but the systems were too small to determine its asymptotic form.¹² We have shown that the loop entropy S_{loops} captures the essential features of an entanglement entropy, scaling logarithmically with the subsystem size in 1D and obeying the area law for the 2D Néel state. Being relatively easy to calculate, S_{loops} offers opportunities to study various aspects of entanglement entropy on large spin lattices in other situations of great interest, e.g., at unconventional quantum-critical points.^{41,42}

In Sec. III we already commented on the fact that properties such as S_{VB}^2 and S_{loop} that are defined using specific geometrical properties of the transition graphs (i.e., not following directly from a given operator acting on the spins) in the valence bond basis are not necessarily well defined expectation values of some hermitian operators. Indeed, it has recently been shown that the entanglement entropies defined in this way are dependent on exactly how a state is represented in the overcomplete valence bond basis.⁴³ This may suggest that these quantities are ill-defined. However, given a hamiltonian H , the projector QMC method generates the transition graphs in a unique way, independently of the trial state used (which we have also verified explicitly).

The valence-bond projector technique itself is closely tied to the completely generic “loop-operator” representation of the path integral for a singlet state,^{19,44} and therefore the statistical properties of the transition graph loops (including S_{VB}^2 and S_{loop}) are not really tied to the particular QMC scheme, only to the valence-bond basis. The definitions are tied to the hamiltonian, in the sense

that H generates the transition graphs. We can therefore not, in general, evaluate S_{VB}^2 and S_{loop} uniquely just based on an arbitrary state, but first need to find the “parent hamiltonian” of the state (and furthermore, that parent hamiltonian should have short-range interactions only, so that it is unique—support for this generic statement is discussed in Ref. 45), and use it to generate the transition graphs. States defined based on “unbiased” bond superpositions (which includes contributions from all different ways of expressing the state in terms of singlets obeying Marshall’s sign rule), such as the amplitude-product states (and perhaps generalizations of them including bond correlations) can also be studied, as we have done here in a 2D case (and where it is important to note that for such a state with Néel order, we obtained results in good agreement with the projected ground state of the 2D Heisenberg model). In practice, we expect S_{VB}^2 and S_{loop} to be useful primarily in QMC studies of ground states of specific hamiltonians.

In the loop-operator formulation,^{19,44} one can think of clusters of spins (defined by transition-graph loops) as

forming dynamically in imaginary time. The entanglement entropies S_{VB}^2 and S_{loop} correspond to entropy measurements averaged over equal-time “snapshots” of entangled clusters in this time evolution. Exactly how this dynamic aspect relates to the standard wave-function picture of entanglement entropy is not clear at present, but the results obtained in this paper suggest that there should be a close relationship between them.

Acknowledgments

We would like to thank F. Alet, S. Capponi, C. Chamon, M. Hastings, M. Mambrini, R. Melko, and F. Verstraete for useful discussions. YCL acknowledges support from NSC Grant No. 98-2112-M-004-002-MY3 and the Condensed Matter Theory Visitors Program at Boston University. AWS was supported by the NSF under Grant No. DMR-0803510 and also acknowledges travel support from the NCTS in Taipei.

-
- ¹ J. Eisert, M. Cramer, M. B. Plenio, *Rev. Mod. Phys.* **82**, 277 (2010).
² M. Srednicki, *Phys. Rev. Lett.* **71**, 666 (1993).
³ A. Kitaev and J. Preskill, *Phys. Rev. Lett.* **96**, 110404 (2006).
⁴ M. M. Wolf, F. Verstraete, M. B. Hastings, and J. I. Cirac, *Phys. Rev. Lett.* **100**, 070502 (2008).
⁵ M. Levin and X.-G. Wen, *Phys. Rev. Lett.* **96**, 110405 (2006).
⁶ E. Fradkin and J. E. Moore, *Phys. Rev. Lett.* **97**, 050404 (2006).
⁷ J. I. Cirac and F. Verstraete, *J. Phys. A: Math. Theor.* **42**, 504004 (2009).
⁸ L. Tagliacozzo, G. Evenbly, and G. Vidal, *Phys. Rev. B* **80**, 235127 (2009).
⁹ U. Schollwöck, *Rev. Mod. Phys.* **77**, 259 (2005).
¹⁰ A. B. Kallin, I. Gonzalez, M. B. Hastings, R. G. Melko, *Phys. Rev. Lett.* **103**, 117203 (2009).
¹¹ H. Li and F. D. M. Haldane, *Phys. Rev. Lett.* **101**, 010504 (2008).
¹² M. B. Hastings, I. González, A. B. Kallin, and R. G. Melko, *Phys. Rev. Lett.* **104**, 157201 (2010).
¹³ A. W. Sandvik, *Phys. Rev. Lett.* **95**, 207203 (2005).
¹⁴ F. Alet, S. Capponi, N. Laflorencie, and M. Mambrini, *Phys. Rev. Lett.* **99**, 117204 (2007).
¹⁵ R. W. Chhajlany, P. Tomczak, and A. Wójcik, *Phys. Rev. Lett.* **99**, 167204 (2007).
¹⁶ G. Refael and J. E. Moore, *Phys. Rev. Lett.* **93**, 260602 (2004).
¹⁷ F. Alet, I. P. McCulloch, S. Capponi, and M. Mambrini, *Phys. Rev. B* **82**, 094452 (2010).
¹⁸ J. L. Jacobsen and H. Saleur, *Phys. Rev. Lett.* **100**, 087205 (2008).
¹⁹ A. W. Sandvik and H. G. Evertz, *Phys. Rev. B* **82**, 024407 (2010).
²⁰ S. Liang, B. Doucot, and P. W. Anderson, *Phys. Rev. Lett.* **61**, 365 (1988).
²¹ B. Sutherland, *Phys. Rev. B* **37**, 3786 (1988).
²² B. Sutherland, *Phys. Rev. B* **38**, 6855 (1988).
²³ W. Marshall, *Proc. Roy. Soc. A* **232**, 48 (1955).
²⁴ K. S. D. Beach and A. W. Sandvik, *Nucl. Phys. B* **750**, 142 (2005).
²⁵ J. Lou and A. W. Sandvik, *Phys. Rev. B* **76**, 104432 (2007).
²⁶ K. S. D. Beach, *Phys. Rev. B* **79**, 224431 (2009).
²⁷ K. S. D. Beach, arXiv:0709.4487.
²⁸ C. Dasgupta and S.-K. Ma, *Phys. Rev. B* **22**, 1305 (1980).
²⁹ D. S. Fisher, *Phys. Rev. B* **50**, 3799 (1994).
³⁰ F. Iglói and C. Monthus, *Phys. Rep.* **412**, 277 (2005).
³¹ S. Liang, *Phys. Rev. B* **42**, 6555 (1990).
³² A. W. Sandvik, *Phys. Rev. B* **59**, 14157(R) (1999).
³³ P. Fazekas and P. W. Anderson, *Philos. Mag.* **30**, 423 (1974); P. W. Anderson, *Science* **235** 1196 (1987).
³⁴ A. F. Albuquerque and F. Alet, *Phys. Rev. B* **82**, 180408 (2010).
³⁵ Y. Tang, A. W. Sandvik, and C. L. Henley, arXiv:1010.6146.
³⁶ P. Calabrese and J. Cardy, *J. Stat. Mech. Theor. Exp.* (2004), P06002.
³⁷ H. Tran and N. E. Bonesteel, arXiv:0909.0038.
³⁸ H. Casini and M. Huerta, *Nucl. Phys. B* **764**, 183 (2007).
³⁹ S. Ryu and T. Takayanagi, *Phys. Rev. Lett.* **96**, 181602 (2006).
⁴⁰ Y.-C. Lin, F. Iglói, and H. Rieger, *Phys. Rev. Lett.* **99**, 147202 (2007).
⁴¹ T. Senthil, A. Vishwanath, L. Balents, S. Sachdev, and M. P. A. Fisher, *Science* **303**, 1490 (2004).
⁴² A. W. Sandvik, *Phys. Rev. Lett.* **104**, 177201 (2010).
⁴³ S. Capponi, F. Alet, M. Mambrini, arXiv:1011.6530 (unpublished).
⁴⁴ M. Aizenman and B. Nachtergaele, *Comm. Math. Phys.* **164**, 17 (1994).
⁴⁵ F. Verstraete and J. I. Cirac, *Phys. Rev. B* **73**, 094423 (2006).